

# 1 Chemical variability of groundwater samples 2 collected from a Coal Seam Gas exploration well, 3 Maramarua, New Zealand

---

4 MAURICIO TAULIS<sup>A</sup>, MARK MILKE<sup>B</sup>

5 <sup>A</sup> *School of Earth, Environmental and Biological Sciences, Queensland University of Technology, GPO Box*  
6 *2434, Brisbane, Queensland, Australia 400.* Email: mauricio@taulis.com, tel.: +61 7 31384744, fax: +61 7  
7 31381535

8 <sup>B</sup> *Department of Civil and Natural Resources Engineering, University of Canterbury, Private Bag 4800,*  
9 *Christchurch, NEW ZEALAND*

10 **Keywords:** Coal seam gas (CSG), coalbed methane (CBM), groundwater, Waikato, hydrochemistry,  
11 geochemical modelling

## 12 **Abstract**

13 A pilot study has produced 31 groundwater samples from a coal seam gas (CSG)  
14 exploration well located in Maramarua, New Zealand. This paper describes sources of CSG water  
15 chemistry variations, and makes sampling and analytical recommendations to minimize these  
16 variations. The hydrochemical character of these samples is studied using factor analysis,  
17 geochemical modelling, and a sparging experiment. Factor analysis unveils carbon dioxide (CO<sub>2</sub>)  
18 degassing as the principal cause of sample variation (about 33%). Geochemical modelling  
19 corroborates these results and identifies minor precipitation of carbonate minerals with degassing.  
20 The sparging experiment confirms the effect of CO<sub>2</sub> degassing by showing a steady rise in pH while  
21 maintaining constant alkalinity. Factor analysis correlates variations in the major ion composition  
22 (about 17%) to changes in the pumping regime and to aquifer chemistry variations due to cation  
23 exchange reactions with argillaceous minerals. An effective CSG water sampling program can be put  
24 into practice by measuring pH at the well head and alkalinity at the laboratory; these data can later  
25 be used to calculate the carbonate speciation at the time the sample was collected. In addition, TDS  
26 variations can be reduced considerably if a correct drying temperature of 180°C is consistently  
27 implemented.

## 28 **1. Introduction**

29 Coal Seam Gas (CSG) constitutes an emerging source of natural gas currently under  
30 exploration and development in countries like the US and Australia. Similarly, CSG exploration has  
31 been taking place in New Zealand with trial production pods in Huntly, Taranaki, and Kaitangata (CRL  
32 Energy Ltd, 2010). Although in both Australia and New Zealand CSG exploration and development  
33 has been taking place at a considerable pace, there is concern about potential environmental  
34 problems that could arise as a consequence of these operations (Taulis, 2010).

35 CSG is mainly methane gas stored in underground coal seams saturated with groundwater.  
36 The methane gas is adsorbed within the micropore structure of the coals held in by potentiometric  
37 pressure. To extract this gas, producers depressurize the coal seams by extracting large amounts of  
38 water (typically around 40 m<sup>3</sup>/day but sometimes up to 100 m<sup>3</sup>/day). Therefore, water production is  
39 critical for the success of CSG operations. In addition, CSG water chemistry is important as an  
40 exploration tool and to assess potential environmental implications arising from disposal issues.

41 The geochemical signature of CSG waters has been defined by Van Voast (2003) by analysing  
42 the CSG hydrochemistry for different producing basins in the US. The signature consists of high  
43 sodium and bicarbonate concentrations with low calcium and magnesium, and almost nil sulphate.  
44 In addition, high chloride concentrations are possible, and particularly in coal beds that are  
45 intimately associated with marine beds. In general, CSG waters have high alkalinity with  
46 circumneutral pH and their salinity tends to be in the brackish range (2000 < TDS <10,000 mg/L).

47 A few studies have investigated the hydrochemical nature of CSG waters. For example,  
48 Bartos and Ogle (2002) sampled springs, aquifers and CSG wells completed in coal seam aquifers  
49 within the Wyodak-Anderson coal zone to characterize recharge and groundwater flow processes  
50 within the Powder River Basin (PRB). McBeth et al. (2003a; 2003b) studied the water chemistry and  
51 trace element concentrations in discharge points and holding ponds in three Wyoming watersheds.  
52 Rice (2003) studied the chemical and isotopic composition of CSG waters sampled from 3 producing

53 fields targeting the Ferron Sandstone in Utah and noted hydrochemical differences which she  
54 attributed to separate recharge areas, differences in flow paths, and various solute sources. Patz et  
55 al. (2006; 2004) examined the interaction of CSG discharge water with semi-arid ephemeral stream  
56 channels. This was done by sampling three discharge wells and seven sampling sites within the  
57 stream. Similarly, Jackson and Reddy (2007a, b) collected CSG water samples from outfalls and  
58 discharge points from five different Wyoming watersheds and carried out a geochemical analysis to  
59 assess salinity and sodicity implications. In Australia, Golding et al (2010) studied the hydrochemistry  
60 and isotopic composition of CSG waters from Permian coal beds within the Bowen Basin in  
61 Queensland; this enabled them to infer the origin of the water based on the proximity to recharge  
62 areas while considering the effect of folding and faulting. While in all of these studies the  
63 hydrochemistry of CSG waters fits the geochemical signature as described by Van Voast (2003), none  
64 of these focus on understanding the transient variations of samples taken from a single well over  
65 time.

66 Decker (1987) presented the hydrochemistry of 30 CSG water samples from a well  
67 completed in East Divide Creek Unit, Piceance Basin, Colorado collected between 1985 and 1987.  
68 These samples fit the geochemical signature of CSG waters but also exhibit noteworthy  
69 hydrochemical variations over time. Decker (1987) studied these variations using Piper diagrams,  
70 and inferred that they were caused by a combination of true composition changes and random  
71 errors (e.g. sampling and analysis).

72 The Maramarua coalfield is located in the north-eastern part of the Waikato Coal Region, in  
73 New Zealand's North Island. This region is renowned for holding important coal resources within  
74 the Waikato Coal Measures. Since 2003, significant CSG exploration activity has been undertaken in  
75 this region by both the L&M Group and Solid Energy. In 2004, a CSG exploration borehole (C1) in  
76 Maramarua was converted into a CSG pilot test by L&M, and active pumping from this well resulted  
77 in 31 CSG water samples. A preliminary analysis of these samples was presented by Taulis and Milke

78 (2007) but no conclusions as to the nature of hydrochemical variations were presented in that work.  
79 Therefore, the aim of this article is to unveil the nature of CSG water sample variations from the  
80 Maramarua C1 well and to explore the potential implications this could have on co-produced water  
81 sampling and characterization.

## 82 **2. Materials and Methods**

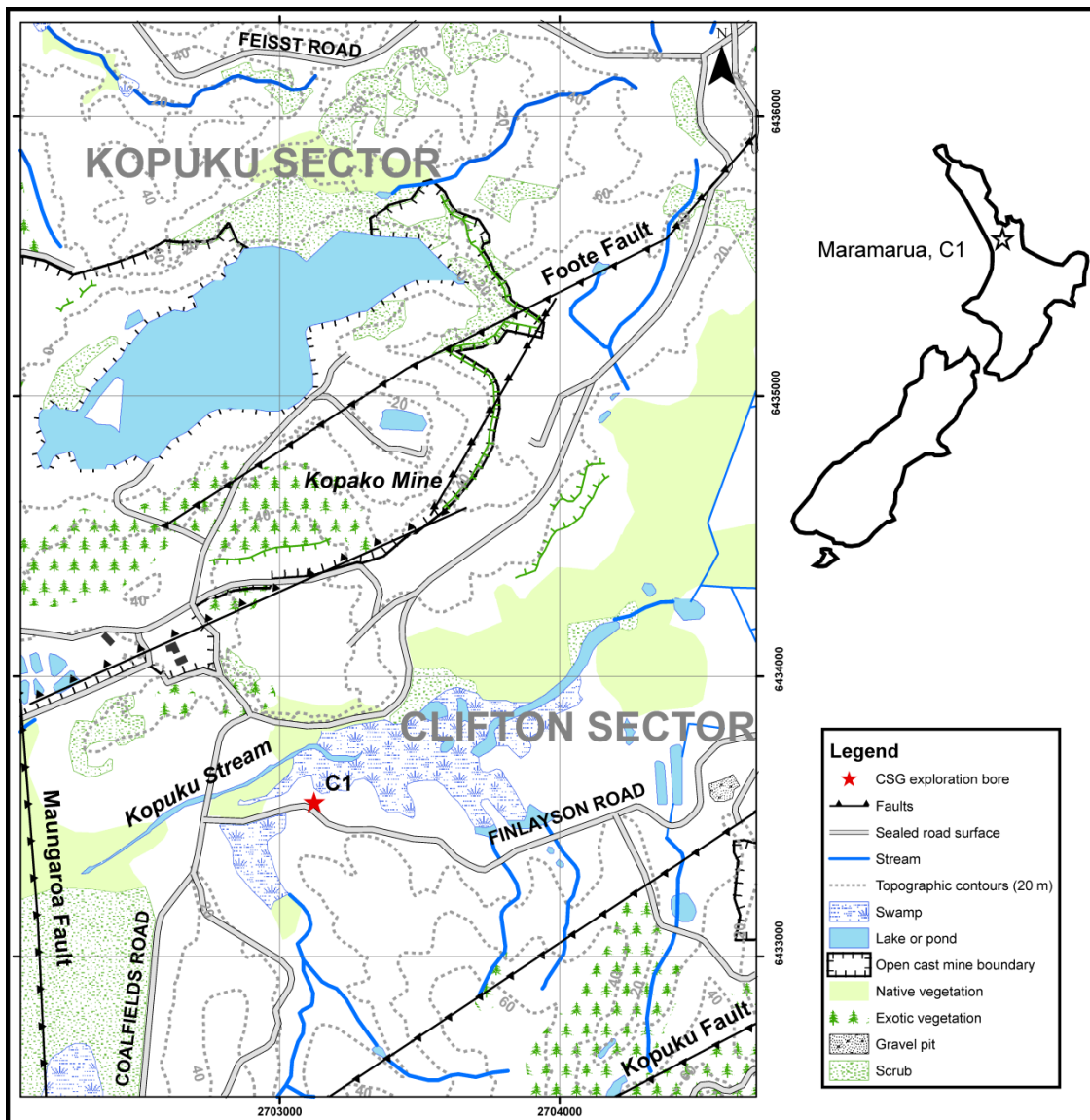
### 83 **2.1 Study Area and CSG Exploration**

84

85 The Maramarua coalfield is bounded by the Maungaroa Fault to the West and by a series of  
86 NE trending normal faults separating it into sectors (Mangatangi, Puketoka, Kopuku, Clifton, and  
87 Maby sectors) (Edbrooke, 1981). The main coal resources are contained within the Waikato Coal  
88 Measures (WCM), deposited in the Eocene, and consisting of carbonaceous mudstones (clay and  
89 shales), sandstone conglomerates, fresh limestone, and sub-bituminous coals. The WCM (0-240m  
90 deep) forms the basement part of the Te Kuiti Group (180 to 600mm thick) which includes estuarine  
91 and shallow marine deposits overlying the WCM (Hall et al., 2006). In August 2003, exploration bore  
92 C1 was drilled in the Kupakupa seam within the Clifton Sector (Figure 1). In June 2004, exploration  
93 hole C1 was fitted with steel casing to carry out the pilot gas test. The casing was set with grout to  
94 about 2 m above the Kupakupa coal seam to isolate it from overlying units (L&M Coal Seam Gas Ltd,  
95 2005) but no screen or gravel pack were fitted at the open interval.

96 Between August and October 2004 pilot testing of the Maramarua C1 borehole produced 22  
97 CSG water samples that were analysed at the EEL (Environmental Engineering Laboratory, University  
98 of Canterbury) . In this particular operation, a “sucker rod” pump was used to pump CSG water to  
99 the surface in order to depressurize the Kupakupa seam. Pumping took place continuously except  
100 for a few interruptions due to pump break downs. Water samples were collected whenever pumping  
101 was resumed and had been ongoing for some period of time. Whenever there was a pump break  
102 down, the water level could remain stagnant inside the well for up to several days; the water level

103 would then slowly rise inside the well (due to artesian pressure), but it would decrease as soon as  
104 the pump was repaired and depressurization operations were resumed. However, pumping  
105 operations were suspended in November 2004 due to ongoing pump problems. Pump testing was  
106 resumed in April 2005 when a Progressive Cavity pump was installed in C1 and, between April and  
107 June 2005, 9 more samples were collected using this pump.



108  
109 **Figure 1. Location of Maramarua C1 well (sourced from Topographic Map BB33 and**  
110 **BC33 North Island, Crown Copyright Reserved and after Edbrooke (1981))**

111 **2.2 Sampling and Analysis**

112

113 Common standards for sampling wells usually involve purging the well and taking the sample  
114 only after removing about 3 well volumes of stagnant water. In the case of C1, the well was purged  
115 continuously throughout the gas test because the aim of the test was to lower the water level (to a  
116 level just above the coal seam). Prior to sample collection, Electrical Conductivity, Dissolved Oxygen,  
117 pH, and Temperature were measured at the wellhead with a YSI-556 calibrated meter. On average  
118 these values were 1274  $\mu\text{S}/\text{cm}$ , 24.6%, 7.8, and 18.3°C. Sample collection was carried out in  
119 untreated 1-liter polyethylene sample bottles. Bottles were prewashed and then rinsed three times  
120 with sample water before collecting each sample. No acidification was carried out because this  
121 would have modified the alkalinity and pH of the samples, and this would have impaired the  
122 subsequent laboratory work for non-metal constituents.

123 The analytical methods used throughout this study were based on APHA standards for most  
124 of the parameters being analysed, except for Sulphate and Chloride which were analysed using  
125 HACH methods. Magnesium was calculated from known hardness and calcium concentrations, and  
126 the carbonate species were obtained by solving the carbonate equilibrium equations using alkalinity,  
127 pH, and specific conductance. In addition, a sample collected on 19/8/2004 was sent to certified  
128 laboratories for a complete analysis including minor ions and trace elements. This sample was  
129 collected in a 1-liter untreated polyethylene bottle for major constituents, and in an acidified 250 ml  
130 bottle for dissolved metals. For the analytical determination of TDS by evaporation, samples were  
131 dried at 180°C (APHA, 1999) but were also dried at 103°-105° C for comparison purposes.

132 The 31 water samples analysed at the EEL are presented in Table 1. These samples exhibit  
133 low concentrations of calcium and magnesium accompanied by high concentrations of bicarbonate  
134 and chloride. Also, the sodium concentrations for these samples are consistently high (average = 313  
135 mg/L). Sulphate levels are generally very low (<2mg/L) and below the detection limit. Specific  
136 conductance (1284-1424  $\mu\text{S}/\text{cm}$ ) is fairly high, and TDS values are in the range of 702-814 mg/L. The

137 low sulphate levels, along with the Na-HCO<sub>3</sub>-Cl chemical signature, is indicative of this well's  
138 potential to produce methane gas (Van Voast, 2003).

139 Figure 2 shows a Piper diagram for these samples. On this diagram, the samples appear  
140 clustered together in specific regions. Figure 3 shows significant variations in calcium and  
141 magnesium concentrations but there are no grounds for discarding these samples as sampling  
142 errors.

143

144

145

146 **Table 1. Samples collected during Maramarua pilot gas test (August, 2004 - June, 2005)**

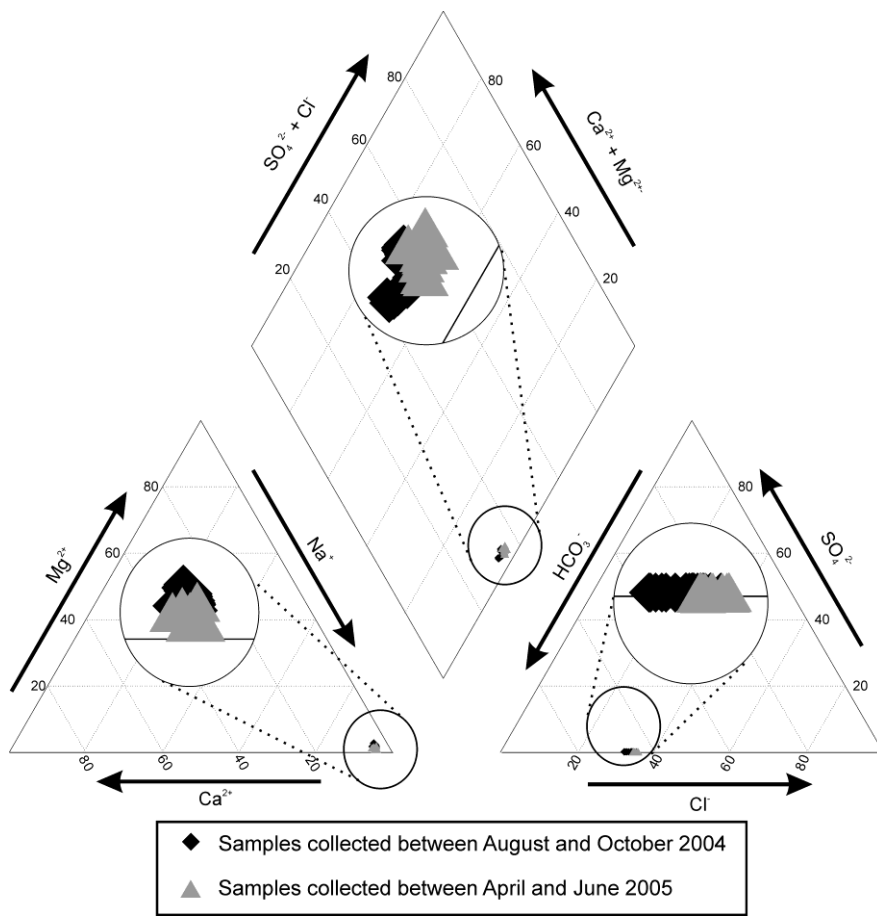
	#	Date	Elapsed time (days)	pH	Sp Cond $\mu\text{S}/\text{cm}$ $T=25^\circ\text{C}$	TDS mg/L	Alkalinity mg/L as $\text{CaCO}_3$	Hardness mg/L as $\text{CaCO}_3$	$\text{Ca}^{2+}$ mg/L	$\text{Mg}^{2+}$ mg/L	$\text{Cl}^-$ mg/L	$\text{SO}_4^{2-}$ mg/L	$\text{HCO}_3^-$ mg/L	$\text{CO}_3^{2-}$ mg/L	$\text{CO}_2(\text{aq})$ mg/L	$\text{Na}^+$ mg/L	WL mbgl
First sampling round	1	01/08/2004	0	7.9	1424	798	428	27.3	7.39	2.13	140	< 2	509.0	2.9	21	326	25
	2	06/08/2004	5	7.9	1390	814	425	29.0	4.48	4.34	142	< 2	512.0	2.9	22	327	40
	3	07/08/2004	6	7.8	1354	786	416	25.0	4.80	3.16	142	< 2	502.6	2.3	26	325	60
	4	08/08/2004	7	7.8	1389	772	413	23.0	4.90	2.62	145	< 2	498.2	2.3	26	317	65
	5	09/08/2004	8	7.8	1386	774	421	25.3	5.32	2.91	142	< 2	509.0	2.2	29	316	70
	6	10/08/2004	9	7.8	1390	702	410	24.8	4.56	3.25	142	< 2	495.6	2.0	29	317	80
	7	16/08/2004	15	7.8	1391	800	394	23.3	5.79	2.13	142	< 2	475.9	2.0	28	311	126
	8	20/08/2004	19	7.9	1357	740	394	32.0	7.79	3.05	143	< 2	474.5	2.6	20	308	55
	9	12/09/2004	41	7.7	1325	742	391	32.7	5.40	4.67	143	< 2	473.4	1.7	32	313	66
	10	13/09/2004	42	7.7	1358	768	388	32.0	5.20	4.63	141	< 2	468.9	1.7	31	308	91
	11	14/09/2004	43	7.7	1380	766	385	30.5	5.20	4.26	141	< 2	465.8	1.7	31	305	100
	12	17/09/2004	46	7.7	1410	786	390	30.5	5.60	4.02	140	< 2	471.9	1.7	31	314	46
	13	18/09/2004	47	7.8	1396	734	390	32.5	4.80	5.00	144	< 2	471.4	2.0	27	311	62
	14	18/09/2004	47	7.8	1418	746	390	31.0	5.00	4.51	142	< 2	471.0	2.1	25	320	64
	15	18/09/2004	47	7.7	1325	772	390	25.0	4.40	3.41	146	< 2	471.9	1.7	32	306	70
	16	19/09/2004	48	7.6	1338	770	388	26.5	4.40	3.78	142	< 2	469.6	1.3	40	309	100
	17	20/09/2004	49	7.6	1361	786	390	26.5	6.39	2.56	146	< 2	472.6	1.3	40	317	105
	18	21/09/2004	50	7.6	1284	792	395	31.5	7.19	3.29	144	< 2	478.7	1.4	40	320	120
	19	04/10/2004	63	7.9	1326	766	390	30.0	6.39	3.41	141	< 2	469.9	2.7	20	318	140
	20	05/10/2004	64	7.9	1380	784	393	28.0	5.99	3.17	148	< 2	472.9	2.7	20	317	150
	21	20/10/2004	79	7.6	1390	746	390	28.0	5.99	3.17	145	< 2	472.6	1.4	40	317	130
	22	21/10/2004	80	7.7	1385	743	390	27.0	5.60	3.17	151	< 2	471.9	1.7	32	318	144
Second sampling round	23	25/04/2005	264	7.2	1270	828	365	28.0	6.40	2.90	145	< 2	443.9	0.5	94	313	70
	24	27/04/2005	266	7.4	1309	812	375	23.0	6.70	1.50	144	< 2	455.4	0.8	61	313	90
	25	29/04/2005	268	7.4	1296	826	378	24.0	5.60	2.40	148	< 2	459.1	0.8	61	308	110
	26	3/05/2005	272	7.5	1309	782	383	19.0	5.20	1.50	143	< 2	464.7	1.0	49	307	130
	27	10/05/2005	279	7.5	1305	784	375	20.0	4.80	1.90	148	< 2	455.0	1.0	48	314	145
	28	23/05/2005	292	7.7	1318	780	383	18.0	4.80	1.50	143	< 2	463.4	1.7	31	312	180
	29	24/05/2005	293	7.4	1296	822	380	29.0	7.90	2.40	143	< 2	461.5	0.8	62	306	60
	30	10/06/2005	309	7.7	1317	844	380	24.0	4.00	3.40	145	< 2	459.8	1.6	31	313	170
	31	11/06/2005	310	7.4	1314	792	380	22.3	4.80	2.50	NA	< 2	461.5	0.8	62	NA	180

Sp Cond = Specific Conductance

WL =depth to water level measured from the surface

mbgl = meters below ground level

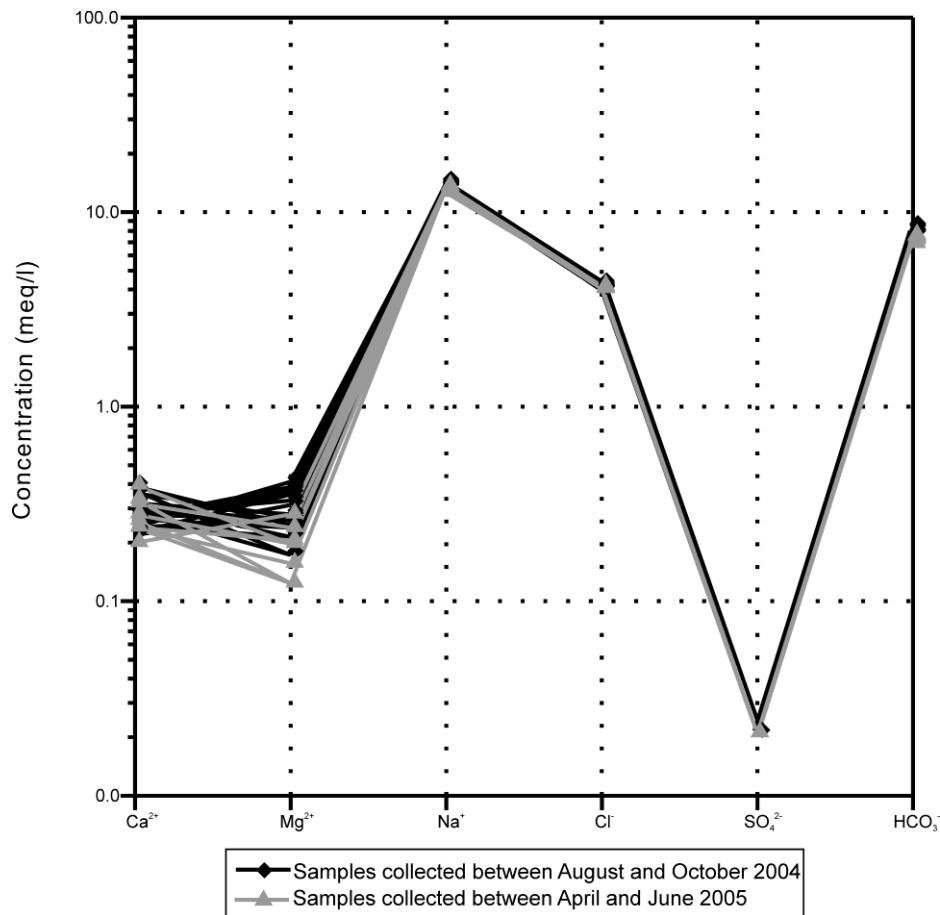




148

149 **Figure 2. Piper diagram for Maramarua C1 samples collected between August, 2004**  
150 **and June, 2005. Sulphate concentrations are plotted as half the detection limit (1 mg/L).**

151



152

153 **Figure 3. Schoeller diagram for Marmarua C1 samples collected between August, 2004**  
 154 **and June, 2005. Sulphate concentrations are plotted as half the detection limit (1 mg/L).**

155

Figure 4 presents the sodium, bicarbonate, chloride, calcium concentrations in water

156

samples along with a plot of water levels, measured during sample collection. An analytical trend

157

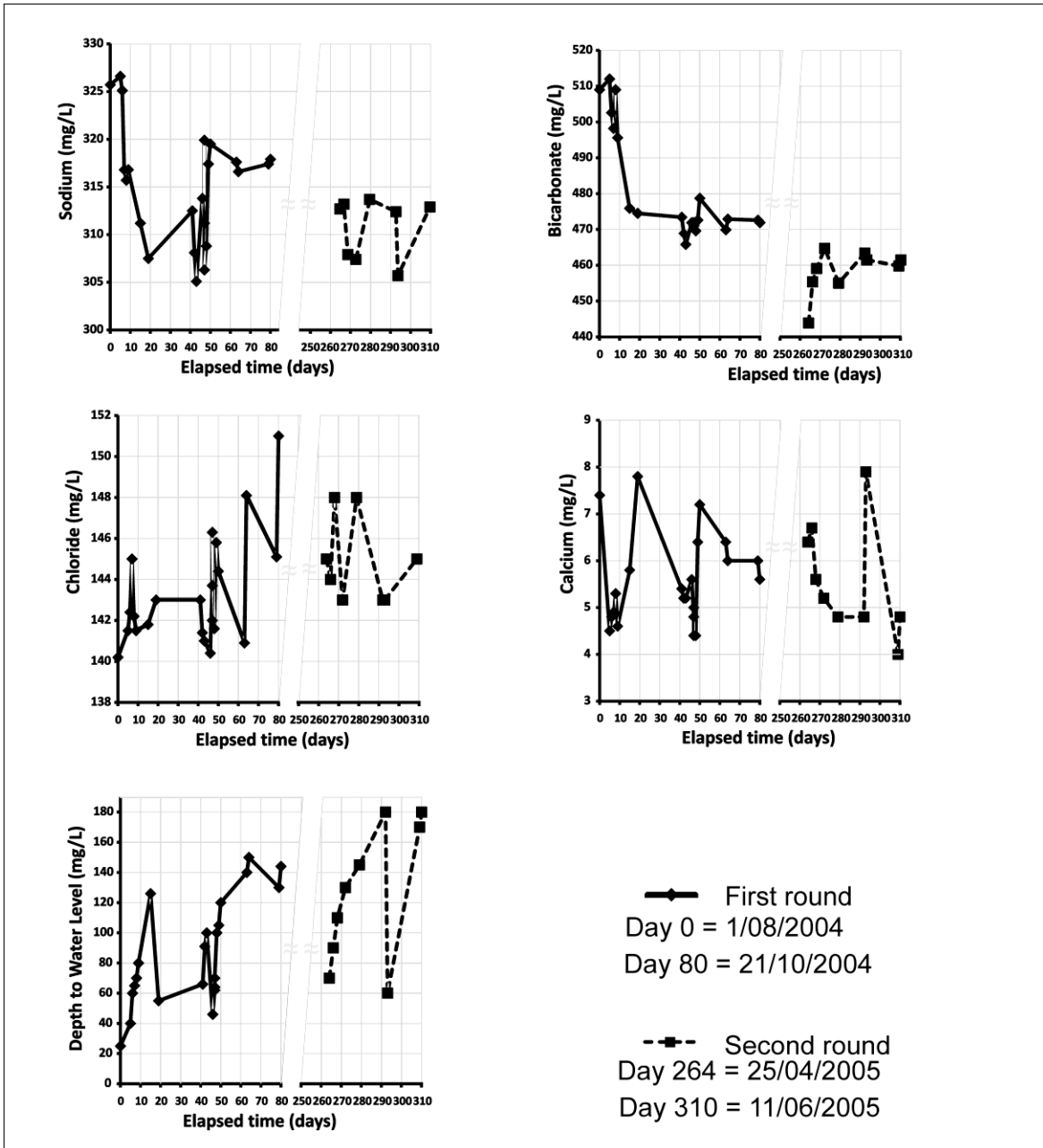
analysis of the data presented here is not straight forward because samples were not collected at

158

equally spaced intervals. In such situations, trend or time-series analysis becomes complicated, and

159

the computation of autocorrelation coefficients is impaired (Chatfield, 1996).



160

161 **Figure 4. Time plots for selected CSG water ions and depth to water level (measured**  
 162 **from the surface)**

163 An idealized representation of the 31 samples collected is presented in Table 2. This table is  
 164 based on average major ion concentrations for the 31 samples presented in Table 1, but with minor  
 165 ions and trace elements from the sample collected on 19/8/2004.

166 **Table 2. Idealized sample using averages of major ions but with minor ions and trace**  
 167 **elements from certified laboratory analyses.**

		Idealized Sample
pH		7.8 <sup>(1)</sup>
Specific Conductance (T=25°C)	µS/cm	1351 <sup>(2)</sup>
TDS	mg/L	776 <sup>(2)</sup>
Hardness	mg/L as CaCO <sub>3</sub>	26.7 <sup>(2)</sup>
Alkalinity	mg/L as CaCO <sub>3</sub>	392 <sup>(2)</sup>
Bicarbonate (HCO <sub>3</sub> <sup>-</sup> )	mg/L	474 <sup>(2,3)</sup>
Carbonate (CO <sub>3</sub> <sup>2-</sup> )	mg/L	1.72 <sup>(2,3)</sup>
Carbon dioxide (CO <sub>2(aq)</sub> )	mg/L	36.8 <sup>(2,3)</sup>
Calcium (Ca <sup>2+</sup> )	mg/L	6 <sup>(4)</sup>
Magnesium (Mg <sup>2+</sup> )	mg/L	0.9 <sup>(4)</sup>
Sodium (Na <sup>+</sup> )	mg/L	314.1 <sup>(2)</sup>
Potassium (K)	mg/L	3 <sup>(4)</sup>
Chloride (Cl <sup>-</sup> )	mg/L	143.7 <sup>(2)</sup>
Sulphate (SO <sub>4</sub> <sup>2-</sup> )	mg/L	0.7 <sup>(1)</sup>
Fluoride (F)	mg/L	0.79 <sup>(4)</sup>
Boron (B)	mg/L	2.5 <sup>(4)</sup>
Silica (SiO <sub>2</sub> )	mg/L	10.7 <sup>(4)</sup>
Total Iron (Fe)	mg/L	0.4 <sup>(4)</sup>
Barium (Ba <sup>2+</sup> )	mg/L	0.024 <sup>(4)</sup>
Zinc (Zn <sup>2+</sup> )	mg/L	1.28 <sup>(4)</sup>

<sup>(1)</sup> Analysed at CRL Energy Ltd Laboratory, Wellington, NZ.

<sup>(2)</sup> Average of 31 samples presented in Table 1

<sup>(3)</sup> Calculated from carbonate equilibrium.

<sup>(4)</sup> Sample was analysed by Hill Laboratories, Hamilton, and NZ.

### 168 2.3 Factor Analysis of hydrochemical data

169 The hydrochemistry of the Maramarua CSG samples was analysed using a form of  
 170 multivariate analysis known as Factor Analysis. Some examples of the application of Factor Analysis  
 171 to hydrochemical studies are given by Liu (2003), Love (2004), and Olmez (1994). Jackson and Reddy  
 172 (2007a) used multi-factor Analysis of Variance to analyse CSG water samples collected from both  
 173 outfalls and discharge ponds to identify differences in physio-chemical properties and ion  
 174 concentrations between watersheds and years, but did not conduct factor analysis to identify  
 175 combinations of variables that control variability.

176 An underlying assumption of factor analysis is that the multivariate data are normally  
 177 distributed (Davis, 2002). Prior to the analysis the data were tested for normality and, in cases  
 178 where the Maramarua CSG water quality data did not follow a normal distribution, transformations

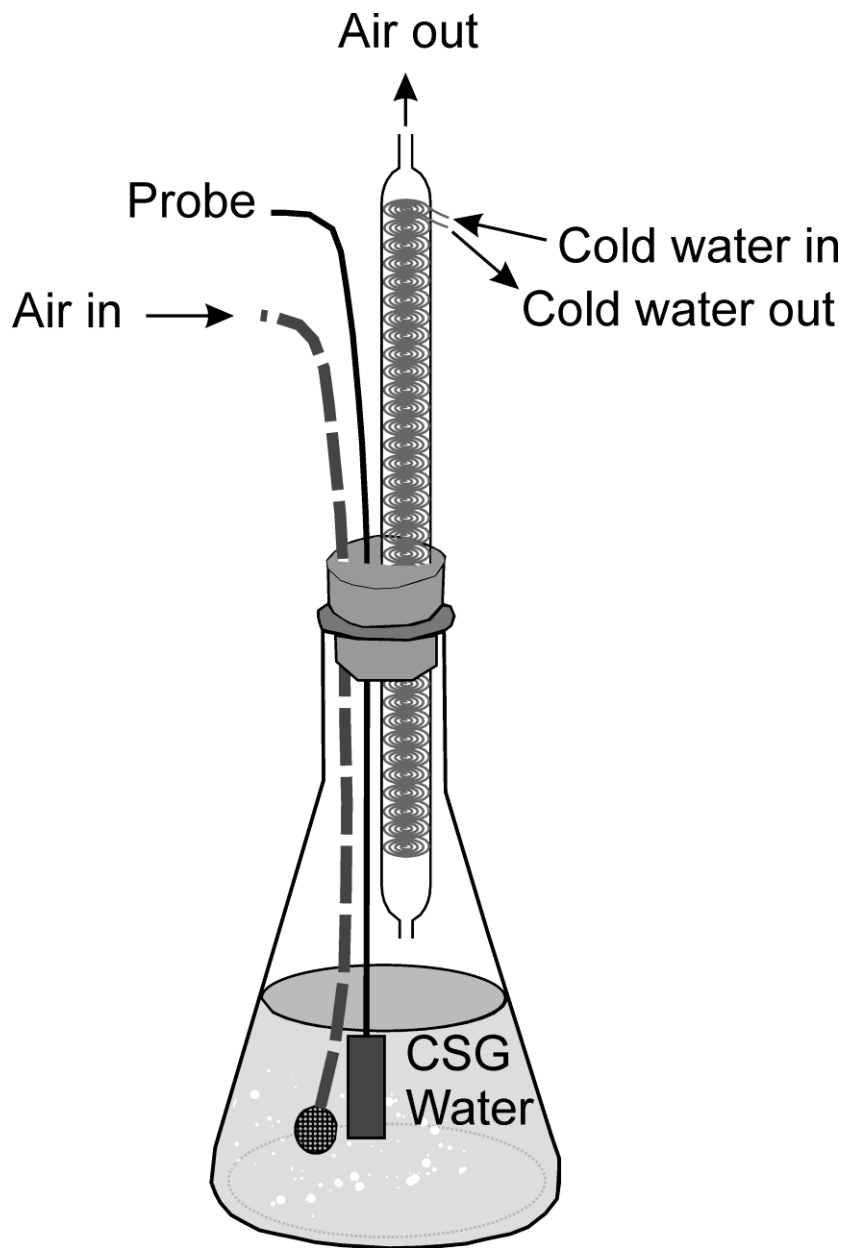
179 were applied so that the data could be analysed using this technique. The Factor Analysis of  
180 Maramarua CSG water quality data was carried out using the MINITAB statistical software package.

181 Maramarua CSG water samples considered for Factor Analysis comprise 31 observations  
182 (samples 1-22 and 23-31 in Table 1). The variables are the chemical properties and constituents  
183 listed in Table 1, including the water levels, but excluding sulphate. However, some of these  
184 variables are either not independent variables or are strongly related to each other (e.g. bicarbonate  
185 and alkalinity, hardness and magnesium) so only independent variables were selected for this  
186 analysis.

## 187 **2.4 Experimental Sparging**

188 A laboratory experiment consisted of sparging the Maramarua CSG water sample collected  
189 on 11/06/2005 to measure hydrochemical changes with degassing. The sample was carefully  
190 analysed (avoiding unnecessary agitation) for specific conductance, alkalinity, pH, hardness, and  
191 calcium. Special provisions were made to measure calcium and hardness – samples were centrifuged  
192 and filtered (using 0.22  $\mu$  filters) to ensure that only soluble ions were measured. Once the sample  
193 was analysed, a 1.5 L sample was placed in a 2 L Erlenmeyer flask. The flask and the water were  
194 weighted prior to starting the sparging experiment. A porous hollow coil was then introduced inside  
195 the flask, and air was continuously pumped through it. A sketch of this experimental setup is  
196 presented in Figure 5. The aim of this experiment was to generate enough air bubbles in order to  
197 cause agitation and accelerate the carbon dioxide degassing process. While the experiment was  
198 being carried out, an open glass column with circulating cold water going through an inner glass coil  
199 (“cold finger”) was introduced into the flask to a level just above the water level mark. This cold  
200 finger acted as a trap for water vapour leaving the system. Water particles leaving the system  
201 condensed on the cold finger and then slowly dripped back into the sample. The opening on top of  
202 the flask was sealed around the cold finger to avoid losses. This sparging experiment was run for 6  
203 hours at a temperature of 20°C. After this time, the flask was weighed and the specific conductance

204 of the sparged water was recorded. Any discrepancies, due mainly to water vapour escaping the  
205 system, were corrected by adding deionized water.



206

207 **Figure 5. Experimental setup for CSG sparging experiment.**

## 208 **2.5 Geochemical Modelling**

209

210 Geochemical modelling of the experimental sparging was carried out using a chemical  
211 speciation model, Visual MINTEQ v. 3.0 (U.S. Environmental Protection Agency, 2005). The idealized

212 sample presented in Table 2 was used as input for the model but using the initial and final pH values  
213 recorded during the sparging experiment.

## 214 3. RESULTS

### 215 3.1 Factor Analysis of hydrochemical data

216 The first 5 eigenvalues account for 90.9% of the total variance, therefore, only 5 factors were  
217 extracted. Therefore, a Factor Analysis with varimax rotation was carried out on 5 extracted  
218 eigenvalues resulting from a traditional Principal Component Analysis (PCA). The sum of the  
219 calculated communalities resulting from the factor extraction process is 90.9% (Table 3), which is the  
220 total variance after the five factors had been extracted and rotated. However, the variance has been  
221 redistributed among these factors so that, for example, the first factor contains 33% of the variance  
222 while the first PCA eigenvalue had 45%. These five factor score coefficients are shown graphically in  
223 Figure 6.

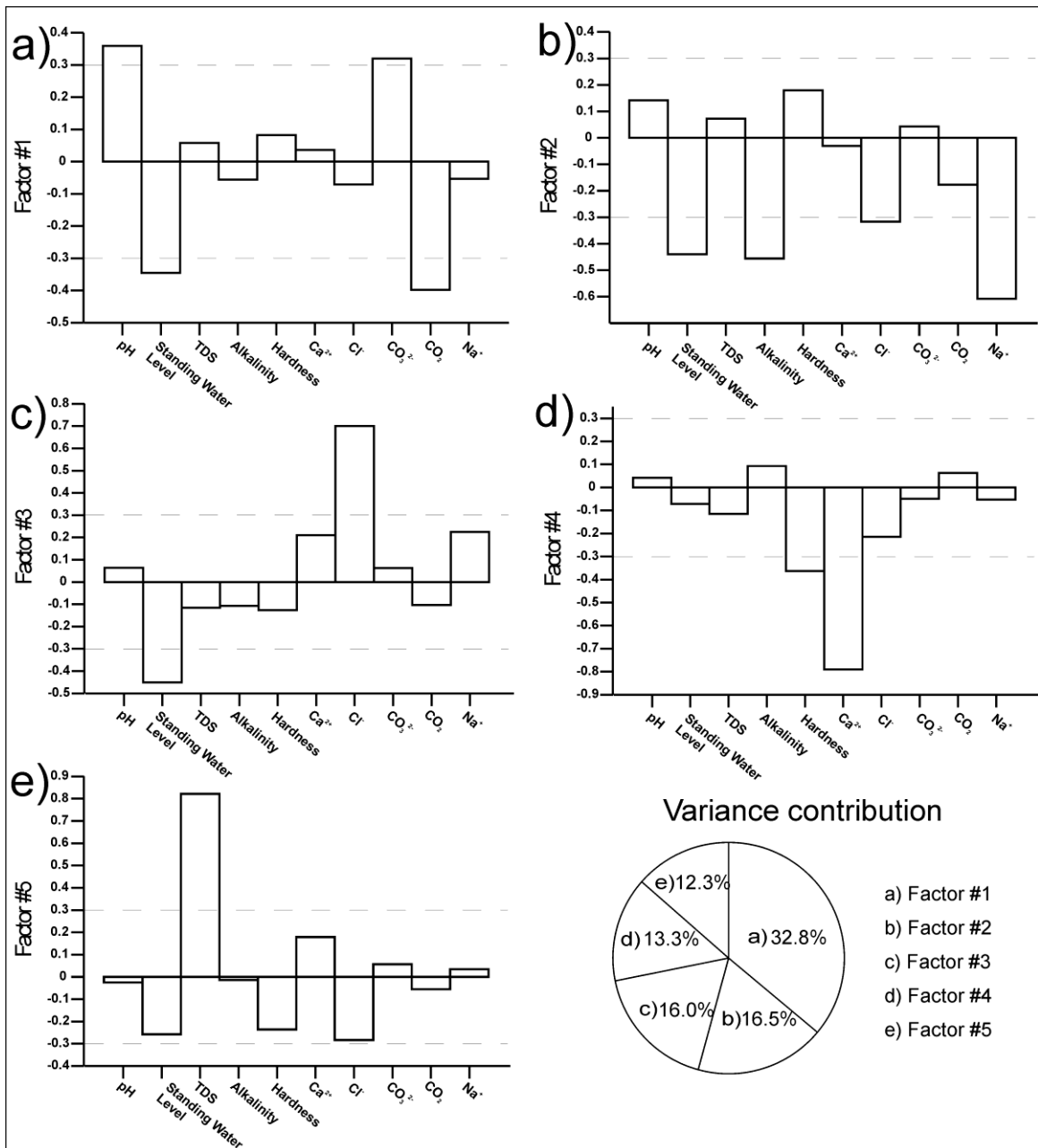
224 **Table 3. Eigenvalues after five factors are extracted**

<b>Factor Score N°</b>	<b>Eigenvalue (<math>\lambda</math>) <sup>(1)</sup></b>	<b>Contribution</b>	<b>Cumulative</b>
<i>B</i> <sub>1</sub>	3.283	32.8%	32.8%
<i>B</i> <sub>2</sub>	1.653	16.5%	49.3%
<i>B</i> <sub>3</sub>	1.596	16.0%	65.3%
<i>B</i> <sub>4</sub>	1.332	13.3%	78.6%
<i>B</i> <sub>5</sub>	1.226	12.3%	90.9%
Total	9.09	90.9%	

<sup>(1)</sup>Eigenvalues for extracted factor score coefficients after varimax rotation

225

226



227

228 **Figure 6. Plot components for factor score coefficients (5 Factors, total variance =**  
 229 **90.9%)**

230 Factor #1

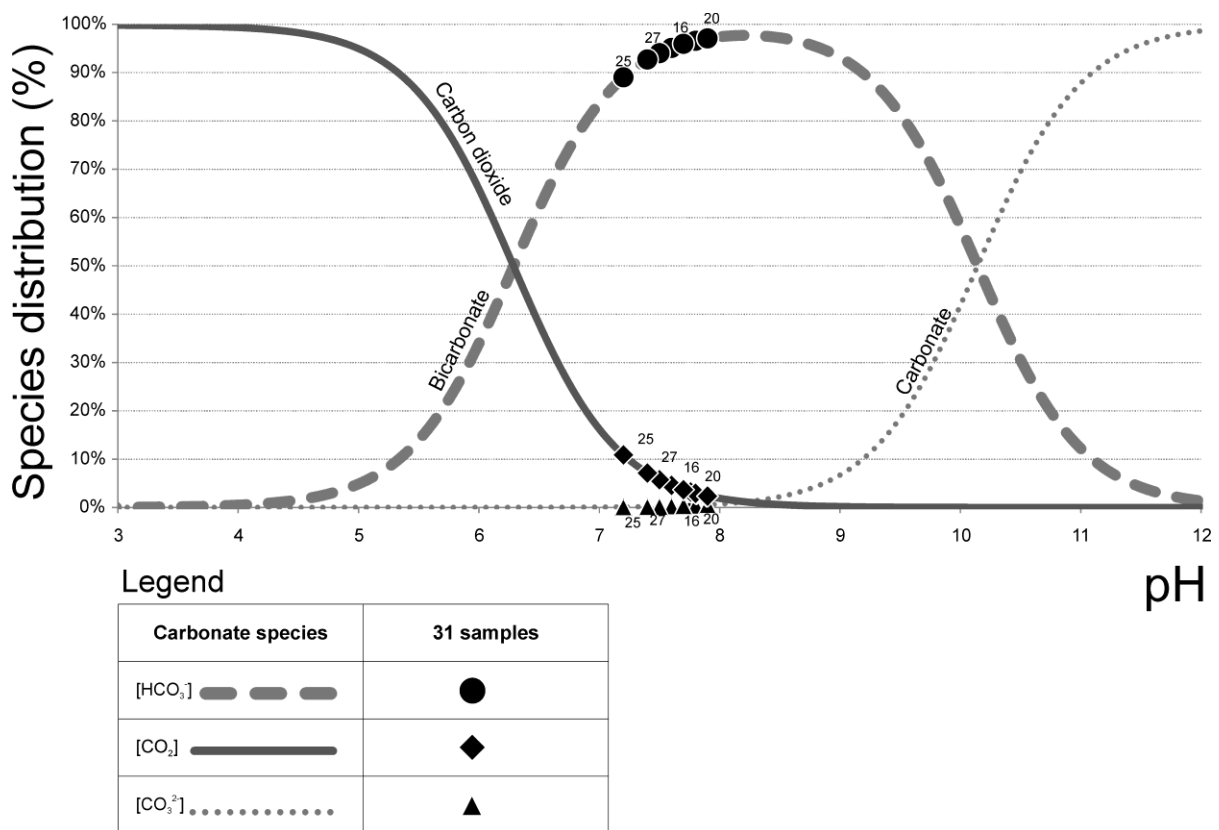
231 The components of the factor score coefficients for the first factor are distributed in such a  
 232 way that only the components for carbon dioxide, pH, water level, and carbonate (in order of  
 233 importance) are significant (e.g. > +0.3 or < -0.3; Figure 6a). This figure indicates that a strong  
 234 decrease in dissolved carbon dioxide tends to be associated with a significant lowering of the water



235 level inside the well together with a considerable increase in pH and carbonate concentrations. This  
236 description fits the carbonate speciation model defined by solving the classical carbonate  
237 equilibrium equations (Freeze and Cherry, 1979; Snoeyink and Jenkins, 1980). To illustrate this point,  
238 these equations were solved for the 31 samples collected, and the resulting species distribution was  
239 plotted on a diagram constructed for different pH values (Figure 7). This plot shows that, for pH  
240 values greater than 7, carbonate concentrations tend to increase with increasing pH values while  
241 carbon dioxide concentrations tend to decrease. The 31 samples do not follow a specific pattern  
242 (some of the earliest samples are clustered together with later samples) and degassing is strongly  
243 correlated against pH. Therefore, the first factor score coefficient represents changes in pH values  
244 resulting from the carbon dioxide degassing process.

245         As the well is depressurized, different samples are collected under different degassing and  
246 agitation conditions. This water may remain inside the well (for a brief period of time) before it is  
247 collected, and the different water levels induce pressure changes, CO<sub>2</sub> degassing, and changes in  
248 hydrochemistry. On the other hand, degassing can also occur by water agitation inside the well (e.g.  
249 turbulent flow due to the absence of a gravel pack) which occurs when the pump is operating at  
250 maximum capacity (e.g. low standing water level), hence the negative value for the component  
251 representing the water level inside the well. Conversely, a low flow rate and a high water level inside  
252 the well could help keep CO<sub>2</sub> in solution as water pressure at the pump intake, located at the bottom  
253 of the well, helps prevent degassing. Therefore, water level variations induce changes in hydraulic  
254 pressure and have a direct impact on CO<sub>2</sub> degassing. During sampling, CSG water samples were  
255 carefully collected by completely filling polyethylene bottles with sample water (to avoid air gaps)  
256 and by sealing the bottles with an air-tight lid. However, when the sample is in a bottle, CO<sub>2</sub>  
257 degassing, carbonate precipitation, and a rise in pH could still occur if the seal is broken or becomes  
258 loose during transport (APHA, 1999). Consequently, the first factor shows that about 33% of the  
259 hydrochemical variations are due to this degassing process either during the sampling of co-  
260 produced water or subsequently during sampling storage and handling.

261 In addition, solving the carbonate system of equations can help describe the degassing  
 262 process at the aquifer level. The lowest pH value detected in the Maramarua CSG water samples was  
 263 7.2 (25/04/2005). Assuming this is the pH of CSG water in the actual coal seam aquifer, the  
 264 carbonate equilibrium equations can be solved with this pH value to calculate aquifer CO<sub>2</sub> partial  
 265 pressure (*p*CO<sub>2</sub>). Using this calculation procedure, it is possible to calculate a *p*CO<sub>2</sub> of at least  
 266 0.012577 atm for the Kupakupa seam at this location. Once this water is exposed to the surface, the  
 267 pressure drops to normal atmospheric levels. Near the coast of New Zealand, for example, the  
 268 atmospheric *p*CO<sub>2</sub> at standard conditions is around 0.000356 atm (Currie et al., 2011). However,  
 269 these changes do not occur instantaneously as revealed by the different pH values in the Maramarua  
 270 CSG water samples.



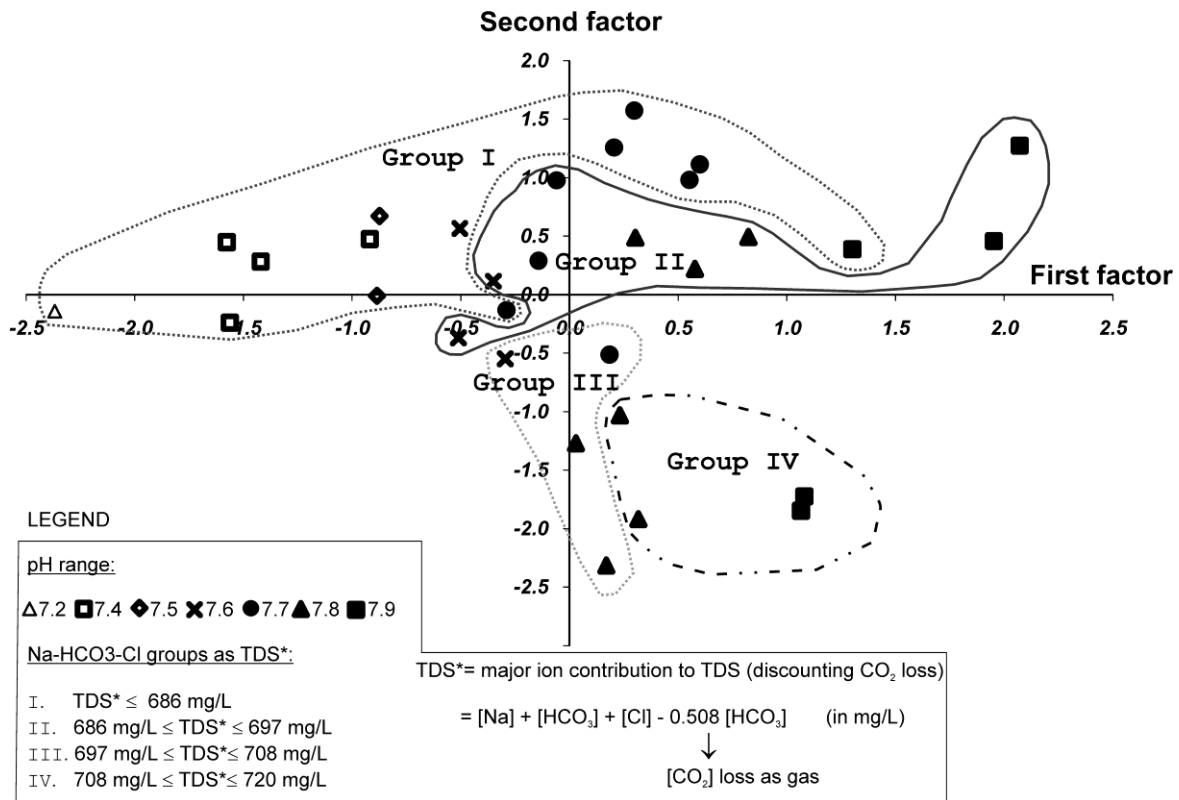
271  
 272 **Figure 7. Distribution of major species of dissolved inorganic carbon for the 31 samples**  
 273 **collected during this study**

274

275 Factor #2

276           The major components in the second factor, which accounts for 16.5% of the variance, are  
277 standing water level inside the well, sodium, alkalinity (equivalent to bicarbonate for the studied pH  
278 range), and chloride (Figure 6b). These ions are the major ions in the CSG water samples collected  
279 throughout the study (water of the Na-HCO<sub>3</sub>-Cl type as illustrated in Figure 2), so this factor is  
280 showing the correlation between the major ion composition and the water level inside the well.  
281 More specifically, this factor shows that with ongoing pumping and thus a low standing water level,  
282 the major ions will have lower concentrations. The second factor is a reflection of mixing processes,  
283 but can also reflect the pumping induced movement of waters of varying composition into the well.  
284 Factor #2 does not contain a TDS (laboratory measurement) term thus indicating that these  
285 variations are not significant enough to affect TDS determinations directly.

286           Figure 8 shows the 31 samples plotted for the first two factors. The symbols represent  
287 sample pH and are labelled according to the major ion contribution to TDS discounting CO<sub>2</sub> loss  
288 (TDS\*), divided in 4 groups. This figure shows that the first factor is strongly linked to pH (from  
289 degassing, see the analysis of Factor #1); pH increases with increasing values for the first factor  
290 scores. The second factor picks up on slight variations in hydrochemistry that occur independently of  
291 pH. Here, factor scores linked to samples with lower TDS\* (Groups I and II) tend to have a positive  
292 value and plot above groups III and IV. These variations in TDS\* are relatively minor but noticeable  
293 enough to explain the significance of the second factor — this factor reveals a correlation between  
294 major ions once corrected for variations due to degassing.



295

296 **Figure 8. Plot of factor scores for the first two factors.**

297

298 Factor #3

299         The third factor (variance contribution =16%) shows a negative correlation between chloride  
 300 and standing water levels in the well (Figure 6c). This complements the interpretation of the second  
 301 factor which showed a positive correlation between chloride and standing water level indicating that  
 302 chloride is one of the major ions present in CSG samples. However, in the case of the third factor,  
 303 the negative correlation between chloride and standing water level would indicate that chloride  
 304 concentrations are high with standing water level decline which is exactly the opposite. Therefore,  
 305 the second and third factors reflect that, although chloride concentrations tend to remain constant  
 306 throughout pumping operations (the relative standard deviation for the 31 samples is 1.8%), some  
 307 variations with pumping are expected. Further chloride variations are likely due to random errors  
 308 associated with analytical determinations (relative error of 1.4% associated with the measuring

309 technique). This factor also reflects the fact that chloride in this CSG water was a less significant  
310 anion (average 4.1 q meq/L) than  $\text{Na}^+$  (13.7 meq/L) and  $\text{HCO}_3^-$  (7.8 meq/L). This aligns with the  
311 stronger weighting on sodium and alkalinity than chloride in factor #2.

#### 312 Factor #4

313 Factor #4 (Figure 6d) shows a strong correlation between calcium and hardness. This is not  
314 unexpected as the value for hardness includes the value for calcium plus the value for magnesium.  
315 Therefore, a strong change in calcium concentrations would cause a change in hardness. The calcium  
316 coefficient for this factor is more heavily weighted than the hardness one (which also includes  
317 magnesium), so calcium is the main source of variation associated to this component. Calcium  
318 concentrations could vary significantly with calcium carbonate precipitation, which occurs with CSG  
319 water degassing. However, factor #4 does not include heavily weighted coefficients for any of the  
320 components associated to calcium carbonate precipitation (pH, standing water level, carbonate, or  
321 carbon dioxide). Since there are no other high-value coefficients for this factor, the calcium variation  
322 expressed by this factor could be attributed to natural variations in calcium in the CSG water  
323 (independent of degassing and the main mineralization processes reflected in Factors #1 and #2) or  
324 to the analytical determination of calcium. APHA (1999) reports a relative standard deviation of 9.2%  
325 associated to this technique, but laboratory titrations conducted could have been as high as 17%.

#### 326 Factor #5

327 In factor #5 (Figure 6e) the only significant component is TDS. Therefore, this factor  
328 represents an independent source of variation associated with the TDS content of the Maramarua  
329 CSG water samples. This variation would be linked to the analytical technique used to measure TDS  
330 rather than to an actual process in the aquifer or within the well. This is because one would expect a  
331 strong correspondence between TDS and the coefficients for the major ions present in the samples  
332 ( $\text{Na-HCO}_3\text{-Cl}$ ), but these coefficients are too low in factor #5. The relative error of TDS

333 determinations could be as high as 7%, so there is a high uncertainty surrounding TDS  
 334 determinations. Consequently, factor #5, which represents 12.3% of the variance, most likely  
 335 represents the uncertainty associated to this measuring procedure.

### 336 3.2 Experimental Sparging

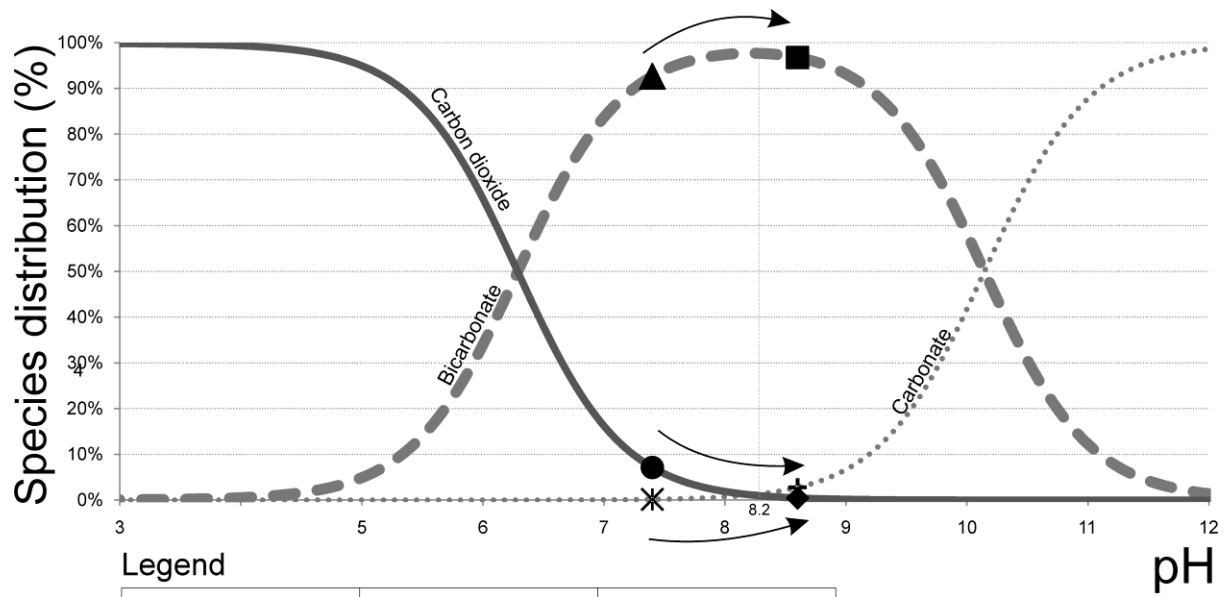
337  
 338 Results for the laboratory sparging experiment are presented in Table 4. After sparging, the  
 339 water was left undisturbed in a closed container for about 8 hours. After this period of time, large  
 340 light grey fragments were observed at the bottom of the bottle. The sample volume was corrected  
 341 by adding 5.57 mL of deionized water to account for water losses through evaporation (0.26%).  
 342 Initial and final conditions after sparging differ mainly in pH, hardness, and calcium concentrations.

343 **Table 4. Sparging experiment results on CSG water sample collected on 11/06/2005**

<b>Parameters</b>	<b>units</b>	<b>prior to sparging</b>	<b>after sparging</b>
Weight (water + flask)	grams	2136.88	2131.31
pH	pH units	7.4	8.6
Specific Conductance	µS/cm	1314	1315
Alkalinity	as mg/L CaCO <sub>3</sub>	380	380
Hardness	as mg/L CaCO <sub>3</sub>	22.3	14.7
Ca <sup>2+</sup>	mg/L	4.8	2.9
Mg <sup>2+</sup>	mg/L	2.5	1.9
HCO <sub>3</sub> <sup>-</sup>	mg/L	461.5	437.7
CO <sub>3</sub> <sup>2-</sup>	mg/L	0.8	12.4
CO <sub>2</sub> (aq)	mg/L	61.7	3.7
H <sub>2</sub> CO <sub>3</sub>	mg/L	0.098	0.006
H <sub>2</sub> CO <sub>3</sub> *	mg/L	61.8	3.7
Saturation Index	pH units	-0.95	0.29

344  
 345 The immediate results from the sparging experiment indicate a rise in pH from 7.4 to 8.6,  
 346 and calcium precipitation in the order of 40%. Hardness is reduced by 34% after sparging, and this is  
 347 mainly a consequence of calcium precipitation. Magnesium precipitation could have also taken place  
 348 (25% at the most), but it is not possible to determine this with certainty because the APHA  
 349 measuring procedure is not sufficiently accurate at such low concentrations.

350           The carbonate species and properties for the 11/06/2005 sample before and after sparging  
351 are presented in Table 4. Before sparging, the major carbonate species was bicarbonate (462 mg/L)  
352 followed by dissolved carbon dioxide (62 mg/L). The calculated  $\text{CaCO}_3$  saturation index for this  
353 sample is negative (-0.95) which means this sample is not precipitating calcium carbonate. Once the  
354 sample was sparged, the carbon dioxide degassing process was accelerated because the sample was  
355 exposed to the open atmosphere and to a lower atmospheric pressure. As a consequence, the pH  
356 rose from 7.4 to 8.6, and the carbonate speciation changed (Table 4). This time, dissolved carbon  
357 dioxide concentrations were very low (3.7 mg/L), and carbonate concentrations increased to 12  
358 mg/L; the major carbonate ion continued to be bicarbonate, but its concentration decreased to 438  
359 mg/L. In general, these results can be interpreted graphically using Figure 9. This figure shows the  
360 shift in the carbonate species' concentrations due to sample sparging. At a pH of about 8.2, the  
361 sparged sample reaches a maximum bicarbonate content in relation to the remaining carbonate  
362 species. As sparging continues, bicarbonate percentage decreases while carbonate increases.  
363 Another significant consequence resulting from sample sparging is the saturation index (Table 4),  
364 which in this case resulted in a positive value (0.29) indicating slight super saturation at the end of  
365 the experiment.



366

367 **Figure 9. Carbonate species prior and after sample sparging**

368



369 **3.3 Geochemical Modelling**

370 MINTEQ results are presented in Table 5. The original sample had a pH of 7.4 and, according  
 371 to MINTEQ, presented some carbonate and zinc precipitation in the form of smithsonite. Calcite,  
 372 carbonate, siderite, and smithsonite precipitation are significant when running the model with a pH  
 373 of 8.6, which corresponds to the pH of the 11/06/2005 sample after the sparging experiment.

374 **Table 5. MINTEQ modelling results**

<b>Modelling of idealized sample with pH = 7.4</b>				
<b>Parameter</b>	<b>total dissolved</b>	<b>%dissolved</b>	<b>total precipitated</b>	<b>% precipitated</b>
Carbonate	$3.90 \cdot 10^{-3}$	99.7	$1.25 \cdot 10^{-5}$	0.3 <sup>(1)</sup>
Zinc	$7.08 \cdot 10^{-6}$	36.1	$1.25 \cdot 10^{-5}$	63.9 <sup>(1)</sup>
<b>Modelling of idealized sample with pH = 8.6</b>				
<b>Parameter</b>	<b>total dissolved</b>	<b>%dissolved</b>	<b>total precipitated</b>	<b>% precipitated</b>
Calcium	$1.0170 \cdot 10^{-4}$	67.9	$4.50 \cdot 10^{-5}$	32.1 <sup>(2)</sup>
Carbonate	$3.8551 \cdot 10^{-3}$	98.4	$6.18 \cdot 10^{-5}$	1.6 <sup>(1,2)</sup>
Iron	$8.2663 \cdot 10^{-7}$	11.5	$6.34 \cdot 10^{-6}$	88.5 <sup>(3)</sup>
Zinc	$1.0100 \cdot 10^{-6}$	5.2	$1.86 \cdot 10^{-5}$	94.8 <sup>(1)</sup>

<sup>(1)</sup>Precipitates as smithsonite (ZnCO<sub>3</sub>)  
<sup>(2)</sup>Precipitates as calcite (CaCO<sub>3</sub>)  
<sup>(3)</sup>Precipitates as siderite (FeCO<sub>3</sub>)

375  
 376 MINTEQ predicted precipitation of calcium (32%), iron ( 89%), and zinc (95%) at pH 8.6.  
 377 MINTEQ shows that CSG waters are undersaturated with respect to carbonate minerals at the  
 378 wellhead (pH =7.4), which suggests these waters do not tend to precipitate carbonate minerals in  
 379 the aquifer. However, once CSG waters reach equilibrium with the atmosphere (pH =8.6), the  
 380 saturation index for most of these minerals (e.g. calcite) increases, and CSG waters tend to  
 381 precipitate carbonate minerals and other minerals (e.g., Fe and Zn) when present.

382 **4. Discussion**

383 As evidenced by Factor #1, when CSG waters are in the aquifer, the aquifer *p*CO<sub>2</sub> can be up  
 384 to two orders of magnitude greater than atmospheric *p*CO<sub>2</sub> at the surface, and the carbonate system  
 385 behaves as a closed system. At this pressure, carbon dioxide will remain dissolved in the water, and

386 the dominant carbonate species will be bicarbonate. Furthermore, CSG waters will be just saturated  
387 or undersaturated. However, once CSG waters are pumped to the surface, the lower atmospheric  
388 pressure will cause carbon dioxide gas to come out of solution and the carbonate equilibrium will  
389 start to change. This observation is in agreement with a study by Patz et al. (2006) in which CO<sub>2</sub>  
390 degassing from CSG water was identified as the likely cause of pH increase in discharge channels  
391 open to the atmosphere.

392 Unless special provisions are taken when collecting a sample (like the use of micropurge sampling  
393 and pressurized flow cells) it is practically impossible to avoid the degassing process.

394 The sample collected on 11/06/2005 from the Maramarua C1 well had unavoidably lost  
395 some carbon dioxide as the water was being pumped to the surface. However, because this sample  
396 was stored in a closed plastic bottle which had been completely filled with CSG water (leaving no air  
397 gaps), the degassing effect was controlled (Saturation Index of -0.95). The saturation index (0.29)  
398 resulting from sample sparging is close to zero because most of the calcite precipitated as carbon  
399 dioxide degassed (it must have been higher at some point but then decreased as calcite  
400 precipitated). This was verified by measuring calcium concentrations before and after sparging with  
401 differences of 40%. In addition, MINTEQ modelling with the idealized sample at pH = 8.6 has resulted  
402 in a positive saturation index, which corroborates the calculated positive saturation index value for  
403 the 11/06/2005 sample after sparging. This shift in the Saturation Index is in agreement with a study  
404 by Jackson and Reddy (2007a) where a decrease in calcium concentrations (e.g. due to calcite  
405 precipitation) was detected in CSG water flowing from outfalls to discharge ponds.

406 Factor analysis shows a correlation between the carbonate precipitation process and water  
407 level fluctuations. In this case, lower water levels imply less hydraulic pressure to keep the CO<sub>2</sub> in  
408 solution. Higher pumping rates lead to both lower water levels and more turbulence, which induces  
409 degassing. Turbulent flow in the zone adjacent to the well and through the pump intake results as a  
410 consequence of well losses. Well losses are generally considered to be proportional to the square of

411 the pumping rate (Jacob, 1946), and these are magnified in absence of a gravel pack which is the  
412 case here.

413           These results highlight the large variations one might find with CSG water due to degassing.  
414 For this CSG water, the true aquifer pH could be as low as 6.6 with a  $p\text{CO}_2$  of 0.037885 atm because  
415 at this pH/ $p\text{CO}_2$  value, MINTEQ predicts no mineral precipitation. However, when CSG water is  
416 abstracted, the pH inside the well immediately begins to rise because of the pressure loss. When  
417 samples are collected, pH could rise further with sample handling. Even if the sample bottle is full  
418 with no air space, degassing will resume upon analysis. The overall time for degassing to occur varies  
419 greatly based on  $\text{CO}_2$  concentrations, temperature, and agitation during storage and transit (APHA,  
420 1999); however, under rigorous sampling and analytical protocols, an analyst might be able to keep  
421 these variations at less than 33%. With poor or variable sampling of CSG water, the resulting data  
422 could have large variations wholly dependent on sampling, analysis procedures, and the amount of  
423 degassing allowed for each sample. To minimize variations due to  $\text{CO}_2$  degassing, APHA (1999)  
424 recommends carrying out laboratory examinations as soon as possible and to analyse samples  
425 promptly after opening the sample container while avoiding vigorous sample agitation. Further  
426 measures can be taken by using a pressurized chamber (e.g. at a pressure equal to the aquifer  $p\text{CO}_2$ )  
427 and to minimize temperature effects (e.g. by keeping the sample at a lower temperature than the  
428 one measured when it was collected).

429           When solving the carbonate system of equations for CSG waters, it is valuable to note that  
430 the addition or removal of carbon dioxide does not influence the final alkalinity value (Snoeyink and  
431 Jenkins, 1980), and this confirms the experimental result in Table 4. Alkalinity could decrease with  
432 calcium carbonate precipitation but calcium concentrations are low in CSG waters to begin with. This  
433 result has further implications for sampling CSG waters – when sampling, it is necessary to measure  
434 pH at the wellhead because this value changes with degassing. Samples can be analysed for alkalinity  
435 at a later stage in the laboratory since this value will not change as carbon dioxide is lost. By

436 measuring alkalinity in the laboratory, and pH in the field, the analyst can reconstruct the true  
437 concentrations before and after degassing. However, pH meters need to be properly calibrated  
438 because, at high alkalinity values (> 400 mg as CaCO<sub>3</sub>/L), pH inaccuracies of 0.1 can result in high  
439 errors (10-15 mg/L for CO<sub>2</sub>) when solving the carbonate equilibrium equations (APHA, 1999).

440           Factor #2 reflects changes in major ion composition with ongoing pumping and lower  
441 standing water levels inside the CSG well. In particular, sodium concentrations tend to decrease with  
442 lower water levels. This is explained by taking into account the different lithologies that give rise to  
443 heterogeneity and confining conditions within the WCM. The WCM are confined by claystones and  
444 present coal seams interbedded with various mudstones (Taulis and Milke, 2007). These  
445 sedimentary rocks contain clay minerals having a significant cation exchange capacity (Domenico  
446 and Schwartz, 1998) hence these minerals tend to adsorb Ca<sup>2+</sup> ions and release Na<sup>+</sup> ions, which  
447 results in CSG waters having high Na<sup>+</sup> concentrations (Van Voast, 2003). Decker (1987) has described  
448 a diffuse layer of cations with high ionic potential (e.g. Ca<sup>2+</sup> and Mg<sup>2+</sup>) bound to clay minerals within  
449 coal measures; in turn, anions with high ionic potential (e.g. CO<sub>3</sub><sup>2-</sup> and SO<sub>4</sub><sup>2-</sup>) will be held more tightly  
450 in the diffuse layer. Because the system must be electrically neutral, this layer will have lower  
451 concentrations of lower ionic potential ions (e.g. sodium, bicarbonate, and chloride). At greater  
452 distances from the diffuse layer, the coal seam aquifer water will not be directly influenced by the  
453 cation exchange capacity of these minerals and the diffuse layer will not be present. When the  
454 pumping rate is increased, after continuous pumping, the standing water level inside the well drops  
455 and the drawdown cone expands. This enables new sites within the coal seam to be accessed and, in  
456 particular, sites adjacent to clay-bearing minerals will be accessed first. Therefore, the diffuse layer  
457 within these sites will be drawn into the well and will mix with other CSG waters. This cation  
458 exchange mechanism could give rise to CSG water having a slightly lower concentration of sodium,  
459 bicarbonate, and chloride but with insignificant changes in salinity (e.g. TDS) as seen with factor #2;  
460 variations due to this effect could be as high as 16.5% independently of degassing effects.

461 Factor#5 has highlighted an important consideration to be taken into account when carrying  
462 out TDS determinations by evaporation. Van Voast (2003) has previously reported laboratory  
463 inconsistencies in the determination of TDS by calculation — the CO<sub>2</sub> that is lost due to evaporation  
464 (about half of the bicarbonate) is not always discounted. When carrying out TDS determinations by  
465 evaporation, APHA (1999) specifies drying temperatures of 180°C for TDS because, when the sample  
466 is dried, CO<sub>2</sub> and H<sub>2</sub>O are lost and bicarbonates are converted to carbonates. However, at  
467 temperatures below 180°C this reaction may not go to completion. This is particularly important  
468 when analysing CSG waters because of the high bicarbonate content present in these waters. Some  
469 laboratories tend to have a relaxed attitude about the drying temperature for TDS and often use  
470 103°-105° C instead of 180°C. This generally would pose no problems in low bicarbonate waters but,  
471 with highly carbonated CSG waters, overestimation of TDS is definitely a possibility. Throughout  
472 these study, samples were dried up at both 103°-105° C and 180°C. It was discovered that TDS values  
473 decreased in about 74% of the samples when using 180°C with values decreasing in about 6% on  
474 average and up to 10% in some cases. Although in this study TDS determinations were carried out at  
475 180°C, random variations in oven temperature or humidity interferences while drying could have  
476 impacted on TDS determinations as shown by factor #5.

477 MINTEQ modelling for the CSG water at this well revealed that degassing is likely to cause  
478 calcium precipitation as calcium carbonate (CaCO<sub>3</sub>) and zinc precipitation as smithsonite (ZnCO<sub>3</sub>).  
479 This last result is in agreement with a study by McBeth et al (2003a) which identified smithsonite  
480 precipitation from CSG water in holding ponds located in the Powder River Basin, Wyoming.  
481 According to MINTEQ, zinc precipitation could be as high as 95% and, in the case of the idealized  
482 sample, which had a zinc concentration of 1.28 mg/L, this could represent a significant reduction  
483 (1.22 mg/L) if the CSG water is exposed to the open atmosphere for some period of time.

## 484 5. Conclusions

485 A pilot CSG well in Maramarua (NZ) has produced water samples exhibiting noteworthy  
486 variations over time. These hydrochemical variations are a product of composition changes induced  
487 by pumping (as high as 50%) and random errors due to sample handling and analysis (as high as  
488 42%).

489 CSG water composition changes induced by pumping are a consequence of both CO<sub>2</sub>  
490 degassing (about 33%) and the mixing of aquifer waters of varying major ion (Na-HCO<sub>3</sub>-Cl)  
491 composition (about 17%). Degassing is an inherent process of pumping but can be controlled with  
492 good production and completion techniques (e.g. gravel pack, continuous pumping, and water level  
493 above the well screen) to promote laminar flow into the well. Continuous pumping at a constant  
494 rate can help minimize variations in major ion composition as water of homogeneous composition  
495 will be drawn into the producing well. Sampling degassing may also occur but these variations can  
496 be minimized by collecting samples with minimum agitation, by filling sample containers completely,  
497 and by using air-tight seals. Degassing prior to analysis can be controlled by transporting the sample  
498 at a low temperature (lower than when it was collected) and by carrying out the analysis as soon as  
499 possible, immediately after opening the sample container.

500 At this well, carbonate minerals likely to precipitate with CSG water degassing were calcium  
501 carbonate (CaCO<sub>3</sub>), smithsonite (ZnCO<sub>3</sub>), and siderite (FeCO<sub>3</sub>). However, concentrations of Ca, Zn,  
502 and Fe tend to be low in CSG waters. Effective sampling of CSG waters can be carried out by  
503 measuring pH with a properly calibrated meter at the well head while carrying out alkalinity  
504 determinations later in the laboratory. These data can then be used to recreate the exact state of  
505 the carbonate species at the time of sample collection. In addition, it is possible to use these data to  
506 infer the *p*CO<sub>2</sub> in the aquifer; in the case of Maramarua C1 this pressure could have been at least two  
507 orders of magnitude higher than atmospheric *p*CO<sub>2</sub>.

508 Random errors due to sample handling and analysis are evident in the determinations of  $\text{Cl}^-$   
509 (16% at the most),  $\text{Ca}^{2+}$  (as high as 13%), and TDS (as high as 12%). Chloride variations could also be  
510 an indication of variations with different pumping regimes, and calcium variations due to this effect  
511 could also be expected. In the determination of TDS by evaporation, it is important to evaporate  
512 samples using the correct drying temperature of 180°C, recommended by APHA (1999), to avoid an  
513 overestimation (as high as 10%) of this parameter. At lower temperatures, bicarbonates may not  
514 completely convert into carbonates, and the evaporation of water and loss of  $\text{CO}_2$  may not fully take  
515 place.

516 CSG waters from Maramarua C1 have a high bicarbonate concentration, which plays an  
517 important role in shaping their hydrochemistry once abstracted. Once exposed to atmospheric  $p\text{CO}_2$ ,  
518 CSG water pH rises considerably, but bicarbonate concentrations will rise while carbon dioxide gas is  
519 vented and carbonate minerals are precipitated. Consequently, different pumping rates, along with  
520 changes in pressure, will yield a continuously changing hydrochemistry.

521

## 522 **References**

- 523 American Public Health Association, American Water Works Association, and Water Environment  
524 Federation., 1999, Standard methods for the examination of water and wastewater:  
525 Washington, D.C., American Public Health Association, 1 computer optical disc p.
- 526 Bartos, T.T., and Ogle, K.M., 2002, Water quality and environmental isotopic analyses of ground-  
527 water samples collected from the Wasatch and Fort Union formations in areas of coalbed  
528 methane development : implications to recharge and ground-water flow, eastern Powder  
529 River Basin, Wyoming. , Water-resources investigations report ; 02-4045: Cheyenne, Wyo;  
530 Denver, CO, U.S. Dept. of the Interior U.S. Geological Survey, p. vi, 88 , (4 folded).
- 531 Chatfield, C., 1996, The analysis of time series : an introduction: London, Chapman & Hall, xii, 283 p.
- 532 CRL Energy Ltd, 2010, Annual Review 2010: Wellington.
- 533 Currie, K.I., Reid, M.R., and Hunter, K.A., 2011, Interannual variability of carbon dioxide drawdown  
534 by subantarctic surface water near New Zealand: Biogeochemistry, v. 104, p. 23-34.
- 535 Davis, J.C., 2002, Statistics and data analysis in geology: New York, J. Wiley, xvi, 638 p. p.
- 536 Decker, A.D., Klusman, R., Horner, D.M., and Anonymous, 1987, Geochemical techniques applied to  
537 the identification and disposal of connate coal water: Proceedings - International Coalbed  
538 Methane Symposium, v. 1987, p. 229-242.
- 539 Domenico, P.A., and Schwartz, F.W., 1998, Physical and chemical hydrogeology: New York, Wiley,  
540 xiii, 506 p.
- 541 Edbrooke, S.W., 1981, Maramarua Coalfield: assessment of exploration 1977-1980., New Zealand  
542 Geological Survey.
- 543 Freeze, R.A., and Cherry, J.A., 1979, Groundwater: Englewood Cliffs, N.J., Prentice-Hall, xvi, 604 p.
- 544 Golding, S.D., Kinnon, E.C.P., Boreham, C.J., Baublys, K.A., and Esterle, J.S., 2010, Stable isotope and  
545 water quality analysis of coal bed methane production waters and gases from the Bowen  
546 Basin, Australia: International Journal of Coal Geology, v. 82, p. 219-231.
- 547 Hall, S.L., Nicol, A., Moore, T.A., and Bassett, K.N., 2006, Timing of normal faulting in the Waikato  
548 Coal Measures, New Zealand, and its implications for coal-seam geometry: New Zealand  
549 Journal of Geology and Geophysics, v. 49, p. 101-113.
- 550 Jackson, R.E., and Reddy, K.J., 2007a, Geochemistry of coalbed natural gas (CBNG) produced water in  
551 powder river basin, wyoming: Salinity and sodicity: Water Air and Soil Pollution, v. 184, p.  
552 49-61.
- 553 Jackson, R.E., and Reddy, K.J., 2007b, Trace element chemistry of coal bed natural gas produced  
554 water in the Powder River Basin, Wyoming: Environmental Science & Technology, v. 41, p.  
555 5953-5959.
- 556 Jacob, C.E., 1946, Drawdown Test to Determine Effective Radius of Artesian Well: Proceeding,  
557 American Society of Civil Engineers, v. 72.



558 L&M Coal Seam Gas Ltd, 2005, PEP 38608 Maramarua Project Report, Ministry of Economic  
559 Development New Zealand. Unpublished Petroleum Report 3212.

560 Liu, C.-W., Lin, K.-H., and Kuo, Y.-M., 2003, Application of factor analysis in the assessment of  
561 groundwater quality in a blackfoot disease area in Taiwan: *Science of The Total*  
562 *Environment*, v. 313, p. 77-89.

563 Love, D., Hallbauer, D., Amos, A., and Hranova, R., 2004, Factor analysis as a tool in groundwater  
564 quality management: two southern African case studies: *Physics and Chemistry of the Earth,*  
565 *Parts A/B/C*, v. 29, p. 1135-1143.

566 McBeth, I., Reddy, K.J., and Skinner, Q.D., 2003a, Chemistry of trace elements in coalbed methane  
567 product water: *Water Research*, v. 37, p. 884-890.

568 McBeth, I.H., Reddy, K.J., and Skinner, Q.D., 2003b, Coalbed methane product water chemistry in  
569 three Wyoming watersheds: *Journal of the American Water Resources Association*, v. 39, p.  
570 575-585.

571 Olmez, I., Beal, J.W., and Villaume, J.F., 1994, A new approach to understanding multiple-source  
572 groundwater contamination: Factor analysis and chemical mass balances: *Water Research*, v.  
573 28, p. 1095-1101.

574 Patz, M.J., Reddy, K., and Skinner, Q.D., 2006, Trace elements in coalbed methane produced water  
575 interacting with semi-arid ephemeral stream channels: *Water Air and Soil Pollution*, v. 170,  
576 p. 55-67.

577 Patz, M.J., Reddy, K.J., and Skinner, Q.D., 2004, Chemistry of coalbed methane discharge water  
578 interacting with semi-arid ephemeral stream channels: *Journal of the American Water*  
579 *Resources Association*, v. 40, p. 1247-1255.

580 Rice, C.A., 2003, Production waters associated with the Ferron coalbed methane fields, central Utah:  
581 chemical and isotopic composition and volumes: *International Journal of Coal Geology*, v. 56,  
582 p. 141-169.

583 Snoeyink, V.L., and Jenkins, D., 1980, *Water chemistry*: New York, Wiley, xiii, 463 p.

584 Taulis, M.E., 2010, Australia and New Zealand CBNG Development and Environmental Implications,  
585 *in* Reddy, K.J., ed., *Coalbed natural gas : energy and environment: Energy science,*  
586 *engineering and technology series.*: New York, Nova Science Publishers, p. xxi, 511.

587 Taulis, M.E., and Milke, M.W., 2007, Coal seam gas water from Maramarua, New Zealand:  
588 Characterisation and comparison to United States analogues: *Journal of Hydrology (New*  
589 *Zealand)*, p. p1-17.

590 U.S. Environmental Protection Agency, 2005, *Exposure Assessment Models*, U.S. Environmental  
591 Protection Agency, p. web page.

592 Van Voast, W.A., 2003, Geochemical signature of formation waters associated with coalbed  
593 methane: *Aapg Bulletin*, v. 87, p. 667-676.

594

595